The Natural Bipeds, Birds and Humans: An Inspiration for Bipedal Robots

Anick Abourachid[1] and Vincent Hugel[2(✉)]

[1] National Museum of Natural History, Paris, France
abourach@mnhn.fr
[2] University of Toulon, Toulon, France
vincent.hugel@univ-tln.fr

Abstract. Despite many studies, the locomotion of bipedal legged robots is still not perfect. All the current robots are based on a humanoid model, which is not the unique one in Nature. In this paper we compare the natural bipedies in order to explore new tracks to improve robotic bipedal locomotion. This study starts with a short review of the historical bases of the biological bipedies to explain the differences between the structures of the human and bird bodies. The observations on the kinematics of bird walking describe a modular system that can be reproduced in robotics to take advantage of the bird leg versatility. For comparison purposes, a bird model is scaled up to have the same mass and the same height of the center of mass as a humanoid model. Simulation results show that the bird model can execute larger strides and stay on course, compared with the humanoid model. In addition the results confirm the functional decomposition of the bird system into the trunk and the thighs for the one part, and the distal part of the leg for the other part.

Keywords: Human bipedy · Bird bipedy · Kinematics · Robotics modeling

1   Introduction

All current operational bipedal robots are humanoid robots. The lower part is either a mobile wheeled base, or is composed of legs with classical kinematics inspired by human legs. Despite progress in locomotion ability, they are quite far from the performances of human locomotion. In this paper, we explore the bipedal systems used in nature in order to find new tracks for improving robots' bipedal locomotion.

The first part presents a short review of the natural bipedal systems, humans and birds, with a short summary of the history and a description of their structure. The second section focuses on the kinematics and dynamics of walking. Section 3 is dedicated to the robotic modeling of both bipeds that are tested on simulations, which are described in Sect. 4. Results are analyzed and discussed in Sect. 5.

The Natural Bipeds

Humans and birds are the only bipedal animals totaling 10001 strictly bipedal species: one species of primate and large diversity of birds. Primates are basically quadruped mammals. Apart from humans, some of them can walk bipedally, but typically in a transitory way, when carrying objects for instance, or for display. Even if humans are able to swim, it is a exceptional behavior, and human are basically specialized for one locomotor behavior: walking. Birds are specialized for the flight, but are also bipedal species. The wings are only used for flying, but the legs are versatile, used for hopping, walking, swimming, but also for take-off and landing. The differences between the natural bipeds arise from different histories. In the primate clade, the permanent bipedal posture appeared 4 million years ago, with the origin of the genus *Australopithecus*. Since then, a bipedal gait was used by seven species of *Homo* over the past 2 million years but is today used exclusively by the species *Homo sapiens*. In contrast, there are 10000 extant representatives of a group of cursorial bipedal dinosaurs, the theropods, that developed the ability to fly during the Mesozoic about 200 million years ago [1]. Some of these flying theropods survived the mass extinction of the dinosaurs and gave rise to the current diversity of birds. All the birds have inherited the same attributes typical of a flying animal and show stick-like forelimbs supporting feathers, a rigid trunk, and a bony short tail [2]. They all have three long bones in the legs: the femur, the tibiotarsus, and the tasometatarsus, and all of them are digitigrade, walking on their toes. The main variability in relation with the locomotor behaviors concerns the development of the sternal keel and the lengths of the wings for flight and the proportions of the leg bones. Depending on the species and their way of life, they vary from 10 to 32 %, 37–56% and 13–45% of the total leg length for the femur, tibiotarsus and tarsometatarsus respectively [3]. On the contrary, all the humans belong to the same species thus the leg proportions are very consistent with the tibia and femur varying up to 6 % of the total leg length among extant populations of humans [4].

The human and bird bodies do not share the same design and geometry (Fig. 1). The human body posture is fully erected, the trunk vertical above the hip on the straight legs. The avian posture is crouched, the joints are flexed, the hips are located on the back, and the trunk is usually hanging horizontally between the thighs. These differences lead to differences in the walking kinematics.

2   Walking in Human and Birds

2.1   Kinematics

The kinematics of human walking can be approximated by an inverted pendulum gait with the moving thigh and the lower leg powering the forward motion of the upper body [5]. The center of mass (CoM) path is guided by adjusting the pelvic rotation, pelvic tilt, lateral pelvic displacement, the knee and hip flexion, and the knee and ankle interaction [6]. The motions of the trunk and the head
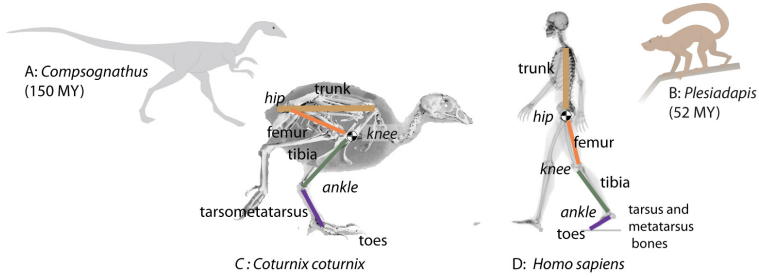
Fig. 1. CoMparison between the two biological bipedal systems. (A) a theropod, close to the birds' ancestor, and (B) a primate, close to the human ancestor, are represented backward. Parts of the body are shared between the birds (C) and the human (D), but the orientation of the segments are different, erected in the humans and crouched in the birds. The 11 bones of the plantar sole, tarsus and metatarsus, included in the human foot, are fused and form the tarsometatarsus bone of the leg in birds. The CoM is at the hip level in humans and at the knee level in birds.

are small and play a minor role in the kinematics compared to the pelvis and legs [6,7]. The arm swing balances the trunk torques induced by the legs [8].

The kinematics of the bird are more versatile as they use more than one loco-motor mode, depending on the species. During walking, the contribution of the thigh to the forward body motion (femur motion) is far lower than that of the more distal segments, the tibiotarsus and the tarsometatarsus [9–11]. The thigh muscles that insert on the pelvis are mainly used to move the trunk that represents 80 % of the body mass, and to adjust the path of the CoM. In terrestrial birds such as the quail (*Coturnix coturnix*), during walking the trunk oscillates around the CoM, pitching, rolling and yawing being guided by the muscles of the thigh that cross the hip [10]. When a duck like the teal (*Callonetta leucophrys*) swims, the part distal to the knee is used as the paddle to propel the system. The thigh does not move at all, anchoring the leg on the trunk similar to a paddle on the hull of a boat. The hip is less flexible compared to that in terrestrial birds such as the quail. Consequently, the thigh is capable of moving the trunk less when walking. The foot is put medially on the ground, allowing medio-lateral translation of the trunk, keeping the CoM above the support polygon. These motions give the typical waddling of ducks [12]. When taking off, the birds hop before using the wings. All the acceleration is provided by the legs, the trunk being propelled first by an extension of the hip joints when the legs push on the substrate [13].

Thus, the birds bipedy may be considered as the association of two morpho-functional modules, the trunk plus thighs guiding the CoM in a different way depending on the species and the locomotor behavior, and the part of the legs distal to the knee, propelling the system. This functional modularity could participate in the versatility of the pelvic locomotor system.

2.2   Dynamics

The comparison of birds with humans shows that in both cases the CoM is at the level of the third joint from the ground up: the hip in humans, the knee in birds. Above the CoM the human trunk is erected and has no significant function in the control of the path of the CoM. In birds, the hip is positioned above the CoM and the thigh muscles can move the trunk to adjust the path of the CoM depending on the mechanical demands. However, during walking, the same mechanism is used in humans and birds to minimize energy expenditure, with a kinetic-gravitational energy transfer during each stride [14]. This mechanism can be modeled by the trajectory of the CoM during locomotion, successively going up and down at each stride like in an inverted pendulum. The relation between the metabolic energy consumption and the mechanical work, as function of speed and body size, is similar in birds, humans and all other mammals [15,16].

Since the two natural biped systems use a dynamic inverted pendulum model during walking, it is possible to use this property to model and to compare both systems. The next sections are dedicated to robotics modeling to test whether a bird-like bipedal robot could be an alternative to a humanoid robot.

3   Robotic Modeling

In order to compare the bird system with the human system, two robotic models were designed for simulation (Fig. 2). The objective is to make these models walk forward inside a dynamic simulator and to check the advantages of the bird system over the human system.

The bird model is inspired by the quail. The leg is composed of three segments – femur, tibiotarsus, and tarsometatarsus, and one main flat toe. The humanoid robotic model is the model used to design the ROMEO humanoid manufactured by the Aldebaran-Robotics company. The model has two segments – femur and tibia–, and one foot per leg. For both models, the CoM, namely G, is placed at the same height $h_G = 0.66$ m (humanoid in flexed position, see simulation Sect. 4). In the bird model, the CoM is located between the knees. The toe length is made larger than the humanoid foot. Actually the toe length was fixed as twice the longitudinal distance between the heel and the knee to ensure the projection of the CoM in the middle of the toe.

Both models have the same mass $m = 40.5$ kg. The mass distribution for the bird model was drawn from a real quail that was frozen and cut into pieces. Each piece was weighed and its CoM was calculated by the double suspension method [17]. In the humanoid model, the CoM is above the hips. The humanoid mass distribution was drawn from the mass distribution of a real human being (Table 1).

The size of the humanoid model is 1.4 m. The size of the bird model is 1.1 m. This size was obtained after scaling up the quail dimensions of the different parts using h_G.

Table 1. Mass rate distribution. For the bird the foot includes the tarsometatarsus and the toes.

	Quail	Humanoid
Head/Neck	9	7.6
Body	63	51
Wings/arms	4×2	5.3×2
Femurs	5×2	9.8×2
Tibias	4×2	4.3×2
Feet	1×2	1.3×2
Total	100	100
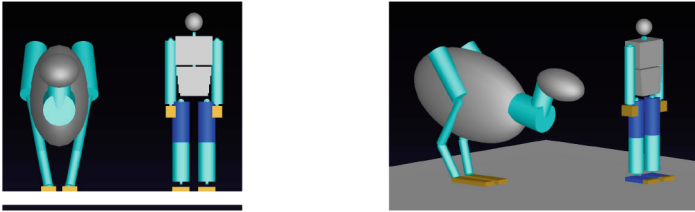
Fig. 2. Robotic models of bird and humanoid.

3.1   Leg Kinematics

The leg of the bird model features two or three rotary joints at the hip, one at the knee, one at the ankle and two joints between the tibiotarsus and the toe, named the foot joint. The hip joints include a roll joint (longitudinal axis), a yaw joint (vertical axis), and a pitch joint (lateral axis) that can be inhibited when necessary to check specific inverse kinematics. The knee joint is a pitch joint (lateral axis) that is slightly rotated in the horizontal plane. The ankle joint is also a pitch joint but with a slight inclination about the longitudinal axis according to the analysis of the quail walk [18]. The foot joint includes a roll joint and a pitch joint.

The humanoid leg has a classical kinematics with three orthogonal rotary joints at the hip – yaw, roll, and pitch joints in this order starting from the pelvis –, a pitch joint at the knee, and a pitch and roll joint at the ankle in this order from the knee [19].

Table 2 summarizes the main characteristic differences between the bird model and the humanoid model. The number of DoF for the bird is set to 6 here since the pitch joint is considered to be inhibited (see simulations). The noticeable differences include the position of the CoM with respect to the hips, the shape of the legs and the distribution of the joint degrees of freedom along the leg.

Table 2. Main characteristic differences between bird and humanoid models.

Characteristics	Bird	Humanoid
Nb of segments/leg	3	2
DoF	6	6
Distribution of DoF (from pelvis)	2-1-1-2	3-1-2
Orientation of joint axes	inclined (knee+ankle)	straight
Legs in standing position	flexed and inclined (knees abducted / feet adducted)	vertically stretched
Location of CoM	middle of knees	above hips
Center-of-mass vertical	through middle of knees	close to frontal plane
Toe/Foot	1 flat main toe (rigid)	1 flat foot (rigid)

3.2   Dynamic Model and Walking Algorithm

The dynamic model adopted for the quail robot and the humanoid robot is the model of the 3D linear inverted pendulum (3D-LIP) where the total robot's mass m is concentrated at the top of a massless stick that joins the Zero Moment Point (ZMP) on the ground to the suspended mass [20,21]. The ZMP can be considered as the center of pressure (CoP) below the supporting foot. The stick is telescopic, i.e. the stick length varies according to the variation of the leg joint angles. The height of the CoM is kept constant during the walk. This means that the humanoid has to flex knees before starting to walk since feet are rigid and remain horizontal during the walk. The bird robot can walk directly without initial configuration. Its feet also remain horizontal. Actually the robotic feet used here are rigid and cannot roll unlike bird toes and human soles.

All the walks have instantaneous double support phases.

The walking algorithm adopted for both models is decomposed into the following steps:

Planning of Forward Foot/Toe Steps. A step is defined as the longitudinal distance between two consecutive feet touching down. The step length is the same along the walk and the first stride is a half step. For all models, the step length was set to 0.25 m for the first set of simulations, then it was set to 0.33 m. The ratio of knee flexion for the humanoid was set to 0.9, this means that the flexion motion leads to the humanoid vertically going down 10 % of the initial hip height. The step duration is the same for all the walks, $t_s = 0.4$ s.

Planning of ZMP. For each support leg, the ZMP is fixed in the middle of the foot/toe when the CoM velocity is constant (no acceleration). The acceleration phase at the beginning of the walk and the deceleration phase at the end were managed separately to calculate the ZMP automatically [21]. At start the ZMP is shifted to the heel, whereas at stop the ZMP is shifted to the front of the foot/toe. This is due to the longitudinal acceleration of the

CoM, which can be tuned by reducing the lengths of the first steps or by increasing the time to execute them.

CoM Trajectory. The horizontal coordinates of the CoM, namely x_G and y_G, are drawn from the equation that govern the linear inverted pendulum model [20]:

$$\ddot{x}_G = \frac{g}{h_G}(x_G - x_P), \quad \ddot{y}_G = \frac{g}{h_G}(y_G - y_P)$$

where g is the gravity and x_P, y_P are the horizontal coordinates of the ZMP. The analytic solution leads to a hyperbolic shape of the CoM trajectory.

Inverse Kinematics. This step is used to calculate the joint commands to be sent to the dynamic simulator. Here the CoM is assumed to be fixed with respect to the trunk of the model, which is a reasonable approximation. The inverse kinematics use the classical pseudo-inverse of the Jacobian matrix that gives the variations of the foot trajectory as a function of the joint angle variations.

4   Simulations

The simulator used is the Adams MSC-Software environment coupled with Matlab. Joint commands are calculated in Matlab and sent to Adams through Simulink using a periodic timer. Joint position and velocity commands are used as desired inputs to PID control blocks inside Adams to control the motors that drive the leg joints. There is no internal stabilizer, i.e. there is no closed-loop control with any inertial measurement unit feedback, because we want to check the suitability of the biped model for the walk using a classical walking algorithm used in robotics.

The interaction model of feet/toes with the ground is achieved through little spherical caps located below the soles of feet/toes. The contact of those caps with the ground result in normal forces that are modeled using penetration depth, penetration velocity, stiffness and damping coefficient [22].

Three kinds of simulations were carried out:

1. humanoid model flexing knees with a flexion ratio of 90 %, then walking 1 m forward with 0.25 m steps lasting 0.4 s each (Fig. 3A).
2. bird model walking 1 m forward with 0.25 m steps lasting 0.4 s each. All hip joints are controlled, and the inverse kinematics process tends to minimize the variations of all joints, and therefore to "distribute" the angle amplitude among all joints (Fig. 3B).
3. bird model walking 1 m forward with 0.25 m steps lasting 0.4 s each. The pitch joint at the hip was inhibited. Consecutively most of the thrusting is achieved by the part of the leg below the knee (Fig. 3C).

The same series of simulation is reproduced with a step length of 0.33 m.

Figure 4 presents the results relative to steps of 0.25 m. The top view figures show the theoretical and real foot(toe)prints, the theoretical trajectory of the
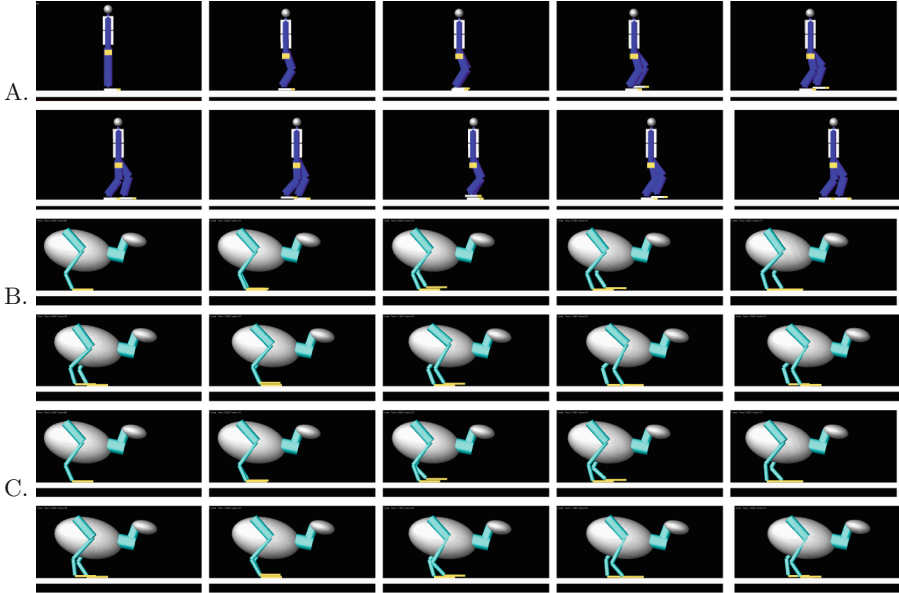
Fig. 3. Successive 0.1 s snapshots of a 1 m forward walking with step length of 0.25 m. A: humanoid model (First 0.7 s of walk after 2 s knee flexion); B: bird model with control of hip pitch joint and C: bird model with hip pitch joint inhibited (First 0.9 s of walk)

CoM, and the centers of pressure and the real CoM obtained from simulation in the dynamic environment. Figure 5 depicts the results relative to steps of 0.33 m. The CoP was calculated at each frame from the normal force sensors located on each spherical cap located on the corners of the feet/toes.

5   Results and Discussion

The results relative to walking steps of 0.25 m show that all models, namely the humanoid, the quail robot with control of the hip pitch joint for walking, and the quail model with the hip pitch joint inhibited, can follow the trajectory of the CoM that was planned offline (Fig. 4).

During the walk the centers of pressure (CoP) of the humanoid model are more scattered than the quail model (Fig. 4A). As long as the CoP remain inside the footprints this is not a problem, however it appears that it is more difficult to stabilize the CoP in the case of the humanoid structure. This observation can be related to the fact that the simulated humanoid can be considered as a double inverted pendulum (leg – trunk with CoM above the hips) actually whereas the simulated quail model can be considered as an inverted pendulum connected to a standard pendulum (leg – trunk with CoM below the hips), which is intrinsically more stable.
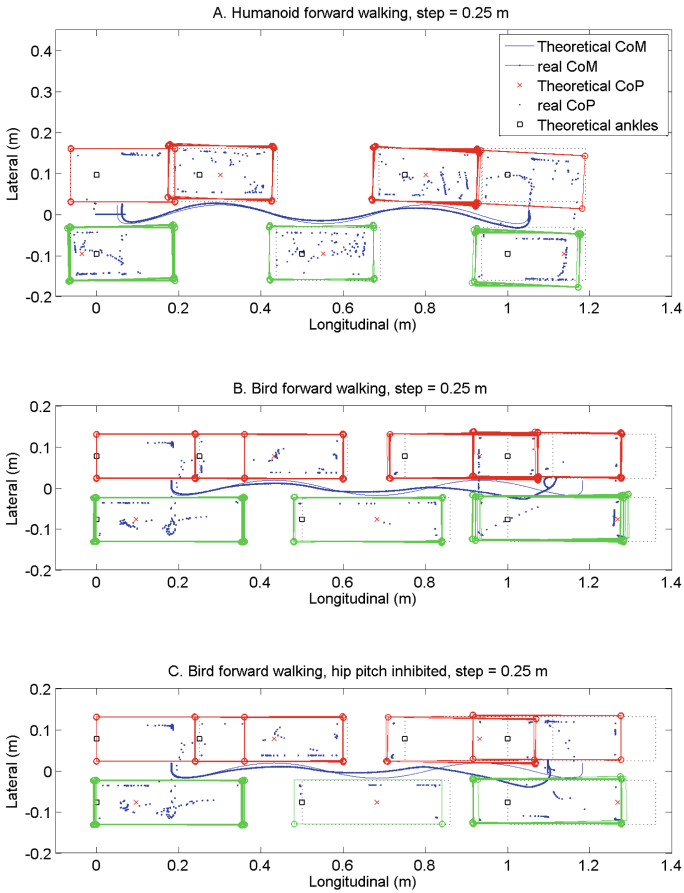
Fig. 4. Footprints of humanoid, and toeprints of bird model walking 1 m forward with step length of 0.25 m. (Color figure online)

It is noticeable that the deceleration phase in the case of the quails leads to little pitching oscillations as a significant number of centers of pressure accumulate on the fore and rear extremities of the toes in the final toeprints (Fig. 4B,C). These oscillations are responsible for a shorter path traveled compared with the path planned, i.e. 0.92 m instead of 1 m. The pitching oscillations can be explained by the fore and rear distributions of the mass of the trunk in the quail model than makes it more sensitive to pitching moves. The quail model with hip pitch joint inhibition is interesting here because the control of the hip pitch joints can be decoupled and used to counteract those pitching oscillations to enhance the walk balance during acceleration/deceleration phases. This matches the observation from biologists that consider that the hip pitch joints play the role of controlling the movement of the trunk with respect to the legs to adjust the posture of the bird.
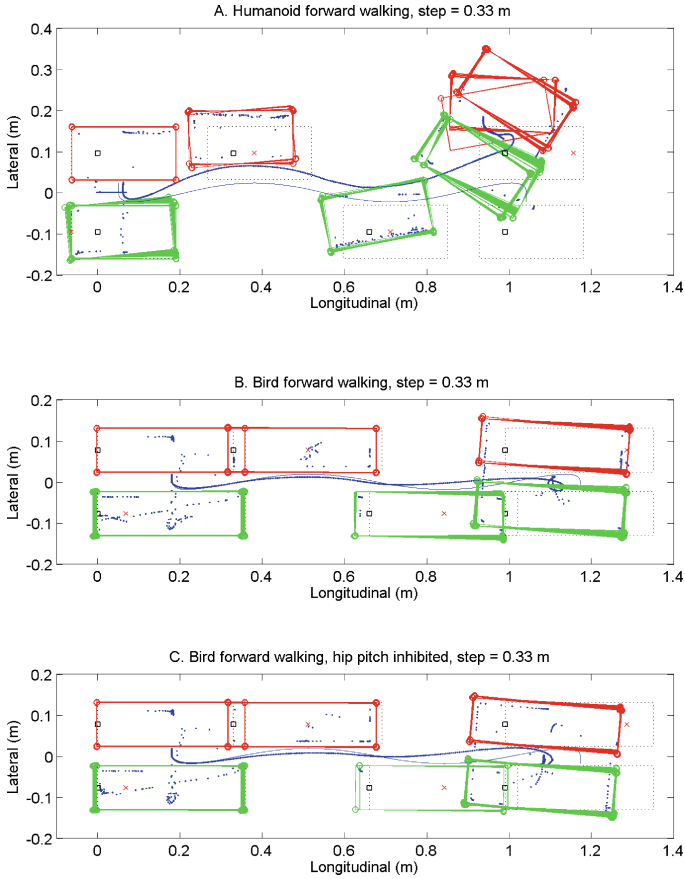
Fig. 5. Footprints of humanoid, and toeprints of bird model walking 1 m forward with step length of 0.33 m. (Color figure online)

The results relative to walking steps of 0.33 m are really selective. Actually the humanoid model cannot stay on course and suffer from disturbing yaw moves from the beginning (Fig. 5A). Centers of pressure accumulate on the lateral sides of the footprints and act as pivots that make the robot turn badly. This highlights the role of the arms in the human walk, whose back-and-forth swing counteracts the disturbing rotation about the vertical. On the contrary the quail model regularly stays on course (Fig. 5B and C) except at the end because the acceleration phase is too fast. The fact that bird legs only account for 20 % of the total mass while human legs account for 30 % diminishes the influence of the disturbing yaw moment due to leg swing in the case of the bird model. This series of simulations shows the superiority of the quail model to achieve larger steps in comparison with the humanoid model of the same mass, with the same height of the CoM. Here it must be noted that the distance between toes in the quail model is smaller than the distance between feet in the humanoid model.

This leads to a reduced amplitude of the oscillation of the CoM in the case of the quail model, which helps the quail model stay on course. Moreover, the real quail adopts a kind of catwalk by placing the landing toe in front of the other support toe, which constrains the amplitude of the CoM sway even more. When scaled up the quail model also features larger toes compared with the humanoid foot size. This difference also contributes to increase the stride range capabilities of the quail model.

The simulation results are interesting but the implementation of the robotic models has some limitations that must be taken into account in the analysis. The first limitation is the walking algorithm that assumes that feet and toes remain flat all along the walk. A consequence is that the humanoid leg and the set of tibiotarsus and metatarsus in the quail model tend to get stretched at the end of the stance phase when the step length is increased, which is not efficient as a starting position to raise the leg, and therefore limits the stride length. This can explain why the natural bipeds roll the foot/toe sole in the stance phase before raising it in order to avoid stretched legs in the rear position. In the case of the humanoid model, the rolling of feet can be useful to avoid the *flexed-knee* walk, and to set up human-like walks with folding and unfolding legs.

In addition the walking algorithms do not include a specific management of the starting and ending phases of the walk. In cruise mode the CoP is planned to stay in the middle of the footprint but in the starting phase the CoP is pushed backwards to initiate the walk, and in the end phase, the CoP is pushed forwards to halt the motion. At last the joints modeled in the dynamic simulator are rigid. There is no flexible joint, neither compliance to store/restore energy as occurs in the natural biped legs.

6   Conclusion

This study has described the biological differences between the human bipeds and the bird bipeds, from a kinematics and a dynamics point of view. Based on these observations, a robotics humanoid model and a robotic quail-like model were designed to compare the walking capabilities of both structures. Simulations carried out inside a dynamic environment have highlighted a major capability of the quail model over the humanoid model, namely the capability to increase the stride length while maintaining the course. Besides, the control of the hip pitch joint in the quail model can be decoupled and used to counteract the pitching oscillations of the trunk in the sagittal plane, the part of the bird leg below the knee being dedicated to thrusting the system. This confirms the mechanical advantage of the modular organization of the bird's bipedy with a trunk-thigh module and a distal module.

Future work will explore the mechanical consequences of the differences in the body proportions observed in birds. Up to now only the ratios of leg segments relative to the quail were used in the simulation study. The limb ratios of other birds could be more suited to the design of a robotic biped. Another research study will focus on the design of rolling toes in order to increase the walking efficiency of the robotic model.

References

1. Hope, S.: The Mesozoic radiation of Neornithes. In: Chiappe, L.M., Witmer, L.M. (eds.) Mesozoic Birds, Above the Head of Dinosaurs, pp. 339–388. University of California Press, Berkeley (2002)
2. Norberg, U.M.L.: Vertebrate Flight. Springer, Berlin (1990)
3. Gatesy, S.M., Middleton, K.M.: Bipedalism, flight and the evolution of theropod locomotor diversity. J Vertebr. Paleontol. **17**, 308–329 (1997)
4. Porter, A.M.W.: Modern human, early human and Neanderthal limb proportions. Int. J. Osteoarchaeology **9**, 54–67 (1999)
5. Pontzer, H., Holloway 3rd, J.H., Raichlen, D.A., Lieberman, D.E.: Control and function of arm swing in human walking and running. J. Exp. Biol. **212**, 523–534 (2009)
6. Hayot, C.: 3D biomechanical analysis of the human walk: comparison of mechanical models. PhD thesis, Poitiers (in French), France (2010)
7. Winter, D., Quanbury, A., Reimer, G.: Analysis of instantaneous energy of normal gait. J. Biomech. **9**, 253–257 (1976)
8. Li, Y., Wang, W., Crompton, R.H., Gunther, M.M.: Free vertical moments and transverse forces in human walking and their role in relation to arm-swing. J. Exp. Biol. **204**, 47–58 (2001)
9. Gatesy, S.M.: Guineafowl hind limb function. I cineradiographic analysis and speed effects. J. Morphol. **240**, 115–125 (1999)
10. Abourachid, A., Hackert, R., Herbin, M., Libourel, P.A., Lambert, F.O., Gioanni, H., Provini, P., Blazevic, P., Hugel, V.: Bird terrestrial locomotion as revealed by 3D kinematics. Zoology (Jena) **114**, 360–368 (2011)
11. Stoessel, A., Fischer, M.: Comparative intralimb coordination in avian bipedal locomotion. J. Exp. Biol. **215**, 4055–4069 (2012)
12. Provini, P., Tobalske, B.W., Crandell, K.E., Abourachid, A.: Transition from leg to wing forces during take-off in birds. J. Exp. Biol. **215**, 4115–4124 (2012)
13. Provini, P., Goupil, P., Hugel, V., Abourachid, A.: Walking, paddling, waddling: 3D kinematics of Anatidae locomotion (Callonetta leucophrys). J. Exp. Zool. **317**, 275–282 (2012)
14. Cavagna, G.A., Heglung, N.C., Taylor, R.: Mechanical work in terrestrial locomotion: two basic mechanisms for minimizing energy expenditure. Am. J. Physiol. **2**, 243–261 (1977)
15. Taylor, C.R., Heglund, N.C., Maloy, G.M.O.: Energetics and mechanics of terrestrial locomotion I Metabolic energy consumption as a function of speed and body size in birds and mammals. J. Exp. Biol. **97**, 1–21 (1982)
16. Fedak, M.A., Heglund, N.C., Taylor, C.R.: Energetics and mechanics of terrestrial locomotion II kinetic energy changes of the limbs and body as a function of speed and body size in birds and mammals. J. Exp. Biol. **79**, 23–40 (1982)
17. Abourachid, A.: Mechanics of standing in birds: functional explanation of lamness problems in giant turkeys. Br. Poult. Sci. **34**, 887–898 (1993)
18. Hugel, V., Hackert, R., Abourachid, A.: Kinematic modeling of bird locomotion from experimental data. IEEE Trans. Robot. **27**(2), 185–200 (2011)
19. Zorjan, M., Hugel, V.: Generalized humanoid leg inverse kinematics to deal with singularities. In: IEEE International Conference on Robotics and Automation, pp. 4791–4796 (2013)
20. Kajita, S.: Humanoid Robot. Ohmsha Ltd, 3–1 Kanda Nishikicho, Chiyodaku, Tokyo, Japan (2005)

21. Hugel, V., Jouandeau, N.: Walking patterns for real time path planning simulation of humanoids. In: IEEE RO-MAN, pp. 424–430 (2012)
22. Zorjan, M., Hugel, V., Blazevic, P., Borovac, B.: Influence of rotation of humanoid hip joint axes on joint power during locomotion. Adv. Robot. **29**(11), 707–719 (2015)